SUPPLEMENTARY INFORMATION (SI)

Insights into the sources of ultrafine particle numbers at six European urban sites obtained by investigating COVID–19 lockdowns

Alex Rowell, James Brean, David C.S. Beddows, Zongbo Shi, Tuukka Petäjä, Máté Vörösmarty, Imre Salma, Jarkko V. Niemi, Hanna E. Manninen, Dominik van Pinxteren, Roy M. Harrison, Thomas Tuch, Kay Weinhold

1. METHODOLOGY

1.1. Sampling Methodologies

Mobility particle size spectrometers (MPSS), including scanning mobility particle sizers (SMPS) and differential mobility particle sizers (DMPS), classify and count particles according to their mobility in an electric field. These systems consist of a charger, a differential mobility analyser (DMA), and a condensation particle counter (CPC). After sampling into the front of the instrument, the charger applies a known equilibrium electric charge distribution to the sampled aerosol population before it is flown into the DMA. The DMA is a cylindrical tube with an electrical field inside it. Voltages are either stepped (DMPS) or scanned (SMPS) across a range which allows a sequence of different particle sizes with different electrical mobilities to reach an exit slit. These size–selected particles can then be counted using a CPC. The CPC exposes these size–selected particles to a supersaturation of vapour (typically butanol) to allow them to grow to optically detectable sizes, before using a light scattering method.

HEL_UB: A custom–built twin–DMPS system with both a TSI 3025 and TSI 3010 particle counter from 3 to 800 nm collects the size distribution data at a time resolution of 10 minutes. The high–flow DMPS channel samples a dried airflow of 3 L min^{-1}, while the low–flow DMPS channel samples a dried airflow of 1 L min^{-1} (Jarvi et al., 2009). Meteorological data were collected on a tower 31 m above ground level at 1–minute time resolution.

LEJ_UB: A custom–built twin–DMPS instrument with TSI 3025 and TSI 3772 CPCs collects the size distribution from 5 to 800 nm in the years 2014–2017 at a time resolution of 10 minutes. In the years 2018–2020, a custom–built SMPS unit with a TSI 3772 CPC collects the size distribution 10–800 nm at a time resolution of 5 minutes. For consistency, the size distribution from 10–800 nm is used from both instruments for the whole period.

BUD_UB: A custom–built flow–switching type DMPS is used with a TSI CPC 3775 particle counter collecting a size distribution from 6 to 1000 nm at 10 minute time resolution (Salma et al., 2016). The system samples a dried sample flowrate of 2.0 L min^{-1} in high flow mode and 0.3 L min^{-1} in low flow mode in accordance with the standard methods of (Wiedensohler et al., 2012). Meteorological data were obtained from regular measurement stations of the Hungarian Meteorological Service operated in Budapest, with a time resolution

of 1–hour (Salma et al., 2016). Traffic census data were measured at 1–hour time resolution also (Salma et al., 2020).

HEL_RS: A custom–built DMPS system with an Airmodus A20 CPC collects the size distribution data from 6 to 800 nm at a time resolution of 10 minutes (Okuljar et al., 2021). The system switches between a dried flowrate of 1 and 4 L min^{-1}. Meteorological data were measured at Pasila weather station approximately 700 m from the measurement station on the roof of an apartment building 53 m a.g.l. Traffic data were taken from a continuous traffic monitoring site approximately 500 m from the Mäkelänkatu supersite.

LEJ_RS: A custom–built twin–DMPS instrument with TSI 3025 and TSI 3772 CPCs collects the size distribution from 10 to 800 nm at a time resolution of 10 minutes between the years 2017–2018. In the years 2019–2020, a custom–built SMPS unit with a TSI 3772 CPC collects the size distribution from 10 to 800 nm at a time resolution of 5 minutes. No auxiliary nor MET data are included here (Birmili et al., 2016).

LDN_RS: An SMPS with TSI 3080 EC, 3081 LongDMA and 3775 CPC collects the size distribution from 16.6 to 604 nm at a time resolution of 15 minutes. The system collects a dried flowrate of 0.3 L min^{-1}.

1.2. Positive Matrix Factorisation (PMF)

The PMF model as applied to size distribution data can be described as follows:

$$X_{ij} = \sum_{k=1}^{p} g_{ik} \cdot f_{kj} + e_{ij} \quad \text{(S1)}$$

where the j^{th} size bin on the i^{th} observation is represented by x_{ij}. The first term on the right–hand side, g_{ik} represents the contribution of the k^{th} factor (of a total of p factors) to the measured number distribution on the i^{th} hour. The second term, f_{kj}, represents the fraction of the j^{th} size bin to the k^{th} factor. The third term, e_{ij}, is the residual for the measurements in the j^{th} size bin on the i^{th} hour. Here, the **G** matrix represents a proxy for the time–series of the strength of source k, and the **F** matrix represents the size distributions produced from source k, sometimes referred to as the source profile. PMF minimises Q which is a function of the sum of squared residuals scaled by their measurement uncertainty, meaning the results are heavily determined by the relative input uncertainties.

Q is defined as:

$$Q = \sum_{i=1}^{m} \sum_{j=1}^{n} \left(\frac{e_{ij}}{s_{ij}}\right)^2 \quad \text{(S2)}$$

where s_{ij} is the input measurement uncertainty of size bin j at time i, and e_{ij} is the model residual of size bin j at time i. Here, PMF is run in *robust mode*, where strong outliers with e_{ij}:s_{ij} > α are reduced to α. In all model runs here, α = 4.

Error estimates are not readily available for SMPS data hence measurement uncertainties are estimated according to previous work (Harrison et al., 2011) from the following equation:

$$s_{ij} = t_{ij} + v_{ij} \cdot max(|x_{ij}||y_{ij}|) \quad \text{(S3)}$$

where x_{ij} are the data values, and y_{ij} are the equivalent data values fitted by PMF. Matrices t_{ij} and v_{ij} are given by

$$t_{ij} = T \cdot (\overline{N_j} + N_{ij}) \quad \text{(S4)}$$

$$v_{ij} = V \quad \text{(S5)}$$

The value of N_{ij} is the number concentration of the size bin j and sample i, and $\bar{N}_j$ is the arithmetic mean of the observed concentration for size bin or gaseous pollutant j. T and V are constants which are varied to seek the natural error in the data, achieving (1) a difference between Q / Q_{theory} = 1 ± 0.01, (2) scaled residuals normally distributed between -3 and 3, and (3) a physically meaningful result. The solution chosen is that with the highest number of physically meaningful factors achievable. Uncertainties in size distribution measurements increase in size ranges <20 nm and >200 nm (Wiedensohler et al., 2012). We therefore increased the values of the T component of the error matrix for these size ranges by 25% to better reflect these unexplainable differences. Between the particle sizing instruments at each site, a common range of 10–600 nm was selected to streamline the analysis. Values for the T component of the error matrix were increased by 200% to ensure the model was being driven by the size distribution most common to all sites. Dependent on availability, hourly means of auxiliary variables, namely, BC, NO_x, O_3, SO_2, $PM_{2.5}$, vehicle count data, and condensation sink, were appended to the input matrix and downweighed in the model by increasing α_j by a factor of 3 to reduce their influence. Where auxiliary variable data were not available, but size distribution data were, the auxiliary data were replaced with their mean values. As these data are downweighed in the model with high uncertainties, this did not affect the factors produced by PMF. Agreement between observed PNC from size distribution measurements and that from recombining the PMF factors (sans residuals) were moderate to substantial at all sites (R^2 between 0.68 – 0.91) (**Figure S2**).

1.3. ECMWF Reanalysis v5 (ERA5)

Meteorological data were taken from the Copernicus ERA climate reanalysis dataset. Meteorological variables, including boundary layer height, global radiation, atmospheric pressure, temperature, and precipitation, were obtained for the relevant lockdown periods at each monitoring site and the equivalent periods in the reference years 2014–2019, depending on data availability.

2. RESULTS AND DISCUSSION

2.1. Identification of Major Factors: Site–by–Site

Below follows a site–by–site description of the major factors identified at each site.

2.1.1. Factors at Helsinki urban background (HEL_UB)

Four factors were identified for HEL_UB. The factors were resolved as nucleation, road traffic$_{svf}$, diffuse urban, and SIA.

Nucleation factor: The size distribution was dominated by a mode of particles peaking at ~12 nm (**Figure S3a**) and the mass distribution was dominated by particles in the accumulation mode (**Figure S3b**). The diurnal profile showed that factor contributions peaked in the early and early afternoon (**Figure S4a**). The factor

exhibited stronger source contributions on weekdays compared to weekends (**Figure S4b**) and had associations with O_3, NO_x, and SO_2 (**Figure 4**). The factor was also associated with low CS (**Figure 4**).

Road traffic$_{svf}$ factor: The size distribution was dominated by a mode of particles peaking at ~35 nm (**Figure S3a**) and the mass distribution was dominated by Aitken and accumulation mode particles (**Figure S3b**). The diurnal profile showed that factor contributions peaked in the early morning and at night (**Figure S4a**). The factor also exhibited stronger source contributions on weekdays compared to weekends (**Figure S4b**) and had associations with NO_x, O_3, and SO_2 (**Figure 4**). The factor is believed to represent road traffic and commercial/domestic activities (such as heating and cooking). Vehicle emissions are likely emanating from on–site parking bays, as well as bordering roadways (from the east; **Figure S5**). Commercial/domestic emissions are likely stemming from university buildings surrounding the research station, as well as large residential areas bordering the site and further afield (from eastern, southern, and westerly directions; **Figure S5**).

Diffuse urban factor: The size distribution was dominated by a mode of particles peaking at ~60 nm (**Figure S3a**) and the mass distribution was dominated by particles in the accumulation mode (**Figure S3b**). The diurnal profile showed that factor contributions peaked in the early morning and at night (**Figure S4a**). Factor contributions were also higher on weekends compared to weekdays (**Figure S4b**) and had associations with NO_x, SO_2, and O_3 (**Figure 4**). The factor is believed to be a represent domestic wood combustion (such as sauna stoves and other fireplaces) and traffic emissions. Traffic rates are notably higher during weekdays, whereas emissions from domestic wood combustion are typically higher during weekends (Luoma et al., 2021).

SIA factor: The size distribution was dominated by a mode of particles peaking at ~160 nm (**Figure S3a**) and the mass distribution was dominated by particles in the accumulation mode (**Figure S3b**). The diurnal profile showed that factor contributions peaked in the early morning and late evening through the night (**Figure S4a**). The factor also exhibited higher source contributions on weekends compared to weekdays (**Figure S4b**) and had associations with O_3, NO_x, and SO_2 (**Figure 4**).

2.1.2. Factors at Leipzig urban background (LEJ_UB)

Four factors were identified for LEJ_UB. The factors were resolved as nucleation, road traffic$_{svf}$, diffuse urban, and SIA.

Nucleation factor: The size distribution was dominated by a mode of particles peaking at ~13 nm (**Figure S3a**) and the mass distribution was dominated by accumulation mode particles (**Figure S3b**). The diurnal profile showed that factor contributions peaked in the early morning, mid–afternoon, and again in the late evening (**Figure S4a**). The factor exhibited stronger source contributions on weekdays compared to weekends (**Figure S4b**) and had associations with O_3, SO_2, and NO_x (**Figure 4**). The factor was also associated with low CS (**Figure 4**).

Road traffic$_{svf}$ factor: The size distribution was dominated by a mode of particles peaking at ~35 nm (**Figure S3a**) and the mass distribution was dominated by particles in the Aitken mode (**Figure S3b**). The diurnal profile showed that factor contributions peaked in the early morning and at night (**Figure S4a**). The factor also

exhibited stronger source contributions on weekdays compared to weekends (**Figure S4b**) and had associations with NO_x, O_3, and SO_2 (**Figure 4**). The factor is believed to represent road traffic and commercial/domestic activities (such as heating and cooking). Road traffic emissions are likely emanating from on–site parking, as well as bordering roadways (from northern and southernly directions; **Figure S5**). Commercial/domestic emissions are likely stemming from buildings within the Science Park, as well as large residential areas bordering the site and further afield (from northern and southernly directions; **Figure S5**).

Diffuse urban factor: The size distribution was dominated by a mode of particles peaking at ~75 nm (**Figure S3a**) and the mass distribution was dominated by particles in the accumulation mode (**Figure S3b**). The diurnal profile showed that factor contributions peaked in the early morning and at night (**Figure S4a**). The factor exhibited stronger source contributions on weekends compared to weekdays (**Figure S4b**) and had associations with NO_x and SO_2 (**Figure 4**). The factor is believed to represent residential wood combustion (for supplementary domestic heating purposes) and road traffic emissions.

SIA factor: The size distribution was dominated by a mode of particles peaking at ~240 nm (**Figure S3a**) and the mass distribution was dominated by particles in the accumulation mode (**Figure S3b**). The diurnal profile showed that factor contributions peaked in the early morning and at night (**Figure S4a**). The factor exhibited higher source contributions on weekdays compared to weekends (**Figure S4b**) and had associations with NO_x, O_3, and SO_2 (**Figure 4**).

2.1.3. Factors at Budapest urban background (BUD_UB)

Five factors were identified for BUD_UB. The factors were resolved as nucleation, road $traffic_{svf}$, diffuse urban, O_3–associated SA, and SIA.

Nucleation factor: The size distribution was dominated by a mode of particles peaking at ~14 nm (**Figure S3a**) and the mass distribution was dominated by particles in the accumulation mode (**Figure S3b**). The diurnal profile showed that factor contributions peaked in the early morning, early afternoon, and again in the late evening (**Figure S4a**). The factor exhibited stronger source contributions on weekdays compared to weekends (**Figure S4b**) and had associations with O_3, NO_x, and vehicle count (**Figure 4**). The factor was also associated with low CS (**Figure 4**).

Road $traffic_{svf}$ factor: The size distribution was dominated by a mode of particles peaking at ~30 nm (**Figure S3a**) and the mass distribution was dominated by Aitken and accumulation mode particles (**Figure S3b**). The diurnal profile showed that factor contributions peaked in the early morning, early to mid–afternoon, and again at night (**Figure S4a**). Factor contributions were also higher on weekdays compared to weekends (**Figure S4b**) and had associations with NO_x and vehicle count (**Figure 4**). The factor is believed to represent road traffic and commercial/domestic activities (such as heating and cooking) emanating from the surrounding districts.

Diffuse urban factor: The size distribution was dominated by a mode of particles peaking at ~65 nm (**Figure S3a**) and the mass distribution was dominated by particles in the accumulation mode (**Figure S3b**). The diurnal profile showed that factor contributions peaked in the early morning and at night (**Figure S4a**). The factor

exhibited higher source contributions on weekends compared to weekdays (**Figure S4b**) and had associations with NO_x (**Figure 4**). The factor is believed to represent biomass burning and road traffic.

O_3–associated SA factor: The size distribution was dominated by a mode of particles peaking at ~ 175 nm (**Figure S3a**) and the mass distribution was dominated by accumulation mode particles (**Figure S3b**). The diurnal profile showed that factor contributions peaked in the daytime (**Figure S4a**). The factor exhibited higher source contributions on weekdays compared to weekends (**Figure S4b**) and had associations with O_3, NO_x, and vehicle count (**Figure 4**). The dial pattern paired with high O_3 covariance suggests that the particles may have grown through the condensation of secondary material.

SIA factor: The size distribution was dominated by a mode of particles peaking at ~200 nm (**Figure S3a**) and the mass distribution was dominated by particles in the accumulation mode (**Figure S3b**). The diurnal profile showed that factor contributions peaked in the early morning and again at night (**Figure S4a**). The factor exhibited higher source contributions on weekdays compared to weekends (**Figure S4b**) and had associations with NO_x and O_3 (**Figure 4**).

2.1.4. Factors at Helsinki roadside (HEL_RS)

Five factors were identified for HEL_RS. The factors were resolved as nucleation, road traffic$_{svf}$, road traffic$_{sf}$, O_3–associated SA, and SIA.

Nucleation factor: The size distribution was dominated by a mode of particles peaking at ~11 nm (**Figure S3a**) and the mass distribution was dominated by accumulation mode particles (**Figure S3b**). The diurnal profile showed that factor contributions peaked in the early morning, late afternoon, and again at night (**Figure S4a**). The factor exhibited stronger source contributions on weekdays compared to weekends (**Figure S4b**) and had associations with BC, NO_x, and vehicle count (**Figure 4**). The factor was also associated with low CS (**Figure 4**).

Road traffic$_{svf}$ factor: The size distribution was dominated by a mode of particles peaking at ~25 nm (**Figure S3a**) and the mass distribution was dominated by particles in the Aitken mode (**Figure S3b**). The diurnal profile showed that factor contributions peaked in the early morning, late afternoon, and again at night (**Figure S4a**). The factor also exhibited stronger source contributions on weekdays compared to weekends (**Figure S4b**) and had associations with BC, NO_x, and vehicle count (**Figure 4**). The factor is believed to primarily represent road traffic emissions, however, the presence of particles from commercial/domestic activities cannot be ruled out.

Road traffic$_{sf}$ factor: The size distribution was dominated by a mode of particles peaking at ~55 nm (**Figure S3a**) and the mass distribution was dominated by particles in the Aitken and accumulation mode (**Figure S3b**). The diurnal profile showed that factor contributions peaked in the mid–morning, early evening, and again at night (**Figure S4a**). Factor contributions were also higher on weekdays compared to weekends (**Figure S4b**) and had associations with BC, $PM_{2.5}$, NO_x and vehicle count (**Figure 4**). This factor is believed to primarily represent road traffic emissions, however, an increase in factor contributions from 19:00 pm onwards (after a

spike in contributions assumed to be traffic–related earlier in the evening) suggests the presence of particles from other mobile and/or stationery combustion–related activities.

O_3–associated SA factor: The size distribution was dominated by a mode of particles peaking at ~120 nm (**Figure S3a**) and the mass distribution was dominated by particles in the accumulation mode (**Figure S3b**). The diurnal profile showed that factor contributions peaked in the daytime (**Figure S4a**). The factor exhibited stronger source contributions on weekdays compared to weekends (**Figure S4b**) and had associations with O_3, BC, and vehicle count (**Figure 4**). The dial pattern paired with high O_3 covariance suggests that the particles may have grown through the condensation of secondary material.

SIA factor: The size distribution was dominated by a mode of particles peaking at ~200 nm (**Figure S3a**) and the mass distribution was dominated by particles in the accumulation mode (**Figure S3b**). The diurnal profile showed that factor contributions peaked in the early morning and at night (**Figure S4a**). The factor exhibited higher source contributions on weekdays compared to weekends (**Figure S4b**) and had associations with $PM_{2.5}$, BC, and NO_x (**Figure 4**).

2.1.5. Factors at Leipzig roadside (LEJ_RS)

Four factors were identified for HEL_RS. The factors were resolved as nucleation, road $traffic_{svf}$, diffuse urban, and SIA.

Nucleation factor: The size distribution was dominated by a mode of particles peaking at ~13 nm (**Figure S3a**) and the mass distribution was dominated by particles in the accumulation mode (**Figure S3b**). The diurnal profile showed that factor contributions peaked in the early morning, mid–afternoon, and again in the late evening (**Figure S4a**). The factor exhibited stronger source contributions on weekdays compared to weekends (**Figure S4b**) and was associated with low CS (**Figure 4**).

Road $traffic_{svf}$ factor: The size distribution was dominated by a mode of particles peaking at ~40 nm (**Figure S3a**) and the mass distribution was dominated by particles in the Aitken and accumulation mode (**Figure S3b**). The diurnal profile showed that factor contributions peaked in the early morning and late evening (**Figure S4a**). Factor contributions were also higher on weekdays compared to weekends (**Figure S4b**). The factor is believed to represent road traffic and commercial/domestic activities (such as heating and cooking).

Diffuse urban factor: The size distribution was dominated by a mode of particles peaking at ~80 nm (**Figure S3a**) and the mass distribution was dominated by particles in the accumulation mode (**Figure S3b**). The diurnal profile showed that factor contributions peaked in the early morning and at night (**Figure S4a**). Factor contributions were also significantly higher on weekends compared to weekdays (**Figure S4b**). The factor is believed to represent residential wood combustion and road traffic emissions.

SIA factor: The size distribution was dominated by a mode of particles peaking at ~240 nm (**Figure S3a**) and the mass distribution was dominated by particles in the accumulation mode (**Figure S3b**). The diurnal profile showed that factor contributions noticeably peaked in the early morning and at night (**Figure S4a**). Factor contributions were also higher on weekdays compared to weekends (**Figure S4b**).

2.1.6. Factors at London roadside (LDN_RS)

Four factors were identified for LDN_RS. The factors were resolved as nucleation, road traffic$_{svf}$, road traffic$_{sf}$, and SIA.

Nucleation factor: The size distribution was dominated by a mode of particles peaking at ~22 nm (**Figure S3a**) and the mass distribution was dominated by accumulation mode particles (**Figure S3b**). The diurnal profile showed that factor contributions peaked in the early morning, throughout the afternoon, and again in the early evening (**Figure S4a**). The factor exhibited stronger source contributions on weekdays compared to weekends (**Figure S4b**) and had associations with O_3, NO_x, $PM_{2.5}$ and BC (**Figure 4**). The factor was also associated with low CS (**Figure 4**).

Road traffic$_{svf}$ factor: The size distribution was dominated by a mode of particles peaking at ~40 nm (**Figure S3a**) and the mass distribution was dominated by particles in the Aitken and accumulation mode (**Figure S3b**). The diurnal profile showed that factor contributions peaked in the mid–morning, mid–afternoon, and again in the late evening (**Figure S4a**). Factor contributions were also higher on weekdays compared to weekends (**Figure S4b**) and had associations with NO_x, BC, O_3, and $PM_{2.5}$ (**Figure 4**). This factor is believed to primarily represent road traffic emissions.

Road traffic$_{sf}$ factor: The size distribution was dominated by a mode of particles peaking at ~88 nm (**Figure S3a**) and the mass distribution was dominated by particles in the accumulation mode (**Figure S3b**). The diurnal profile showed that factor contributions were elevated throughout the day (**Figure S4a**). The factor also exhibited stronger source contributions on weekdays compared to weekends (**Figure S4b**) and had associations with BC, NO_x and $PM_{2.5}$ (**Figure 4**). This factor is believed to primarily represent road traffic emissions.

SIA factor: The size distribution was dominated by a mode of particles peaking at ~280 nm (**Figure S3a**) and the mass distribution was dominated by particles in the accumulation mode (**Figure S3b**). The diurnal profile showed that factor contributions noticeably peaked in the early morning and at night (**Figure S4a**). The factor exhibited higher source contributions on weekdays compared to weekends (**Figure S4b**) and had associations with $PM_{2.5}$, NO_x, BC, and O_3 (**Figure 4**).

3. SUPPLEMENTARY INFORMATION: FIGURES

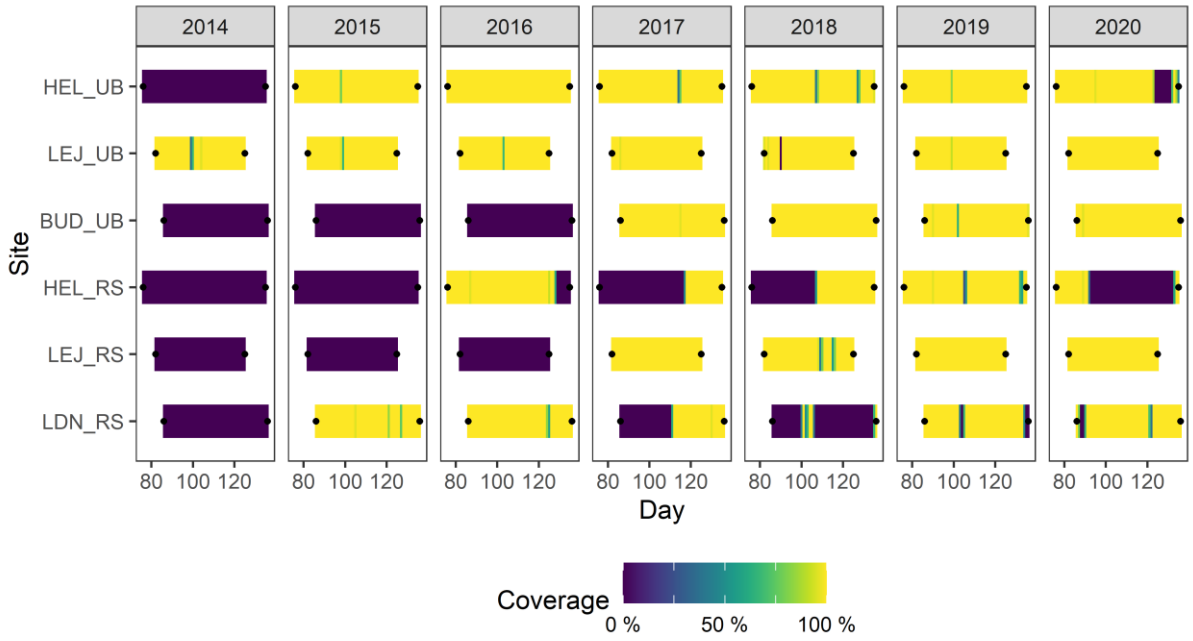

Figure S1: Particle size distribution instrument data coverage during lockdown period and equivalent period for previous years. Each coloured bar represents the percentage data coverage per day. Black dots represent the start and end points of the lockdown periods (Julian Day).

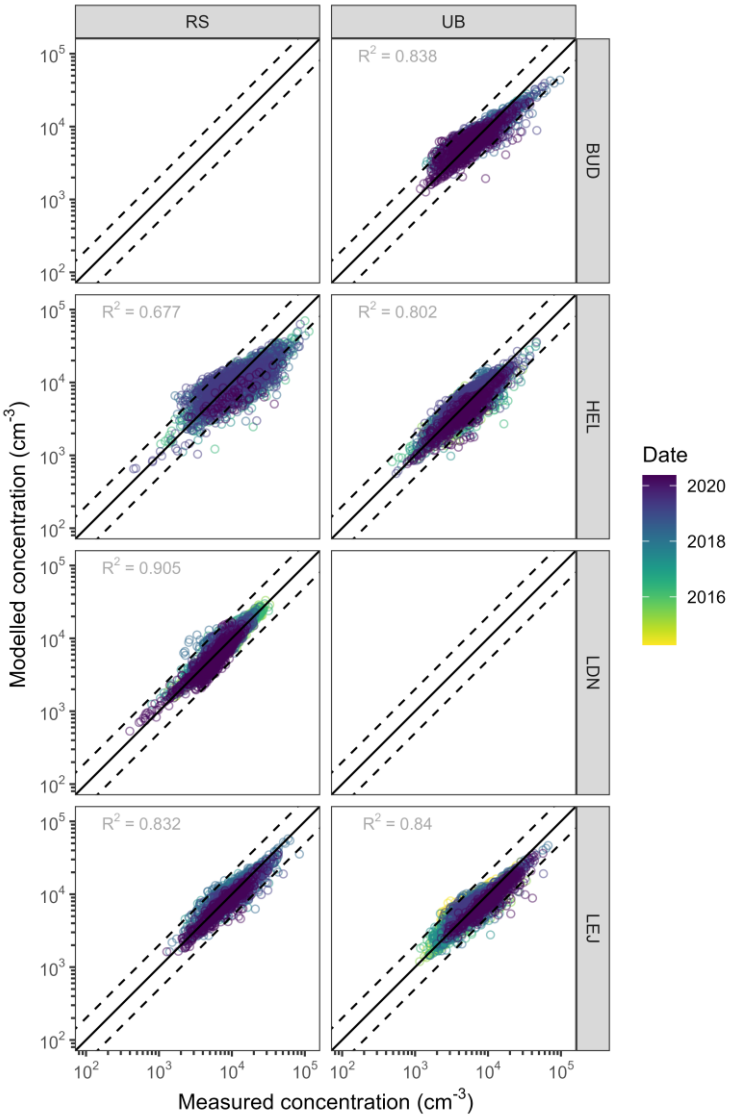

Figure S2: Agreement between observed particle number concentration from size distribution measurements and that from recombining the PMF factors at each site.

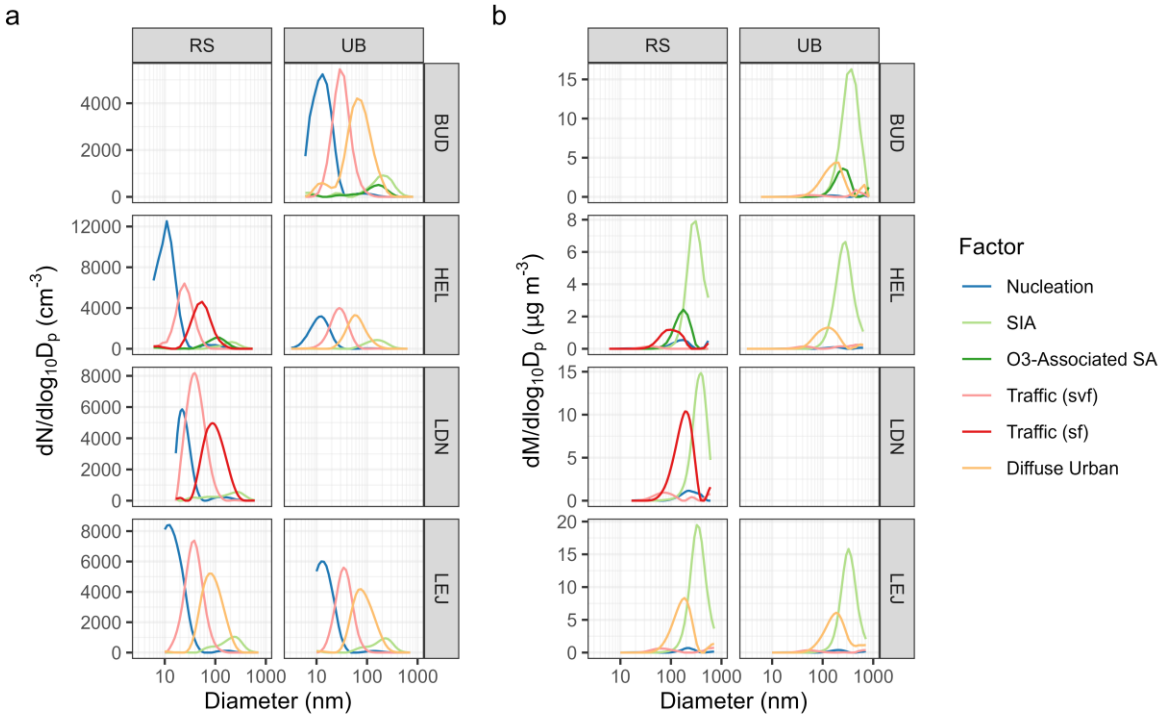

Figure S3: Number (a) and mass (b) size distribution data for each factor at each monitoring site. Each panel represents a site and each colour represents a factor.

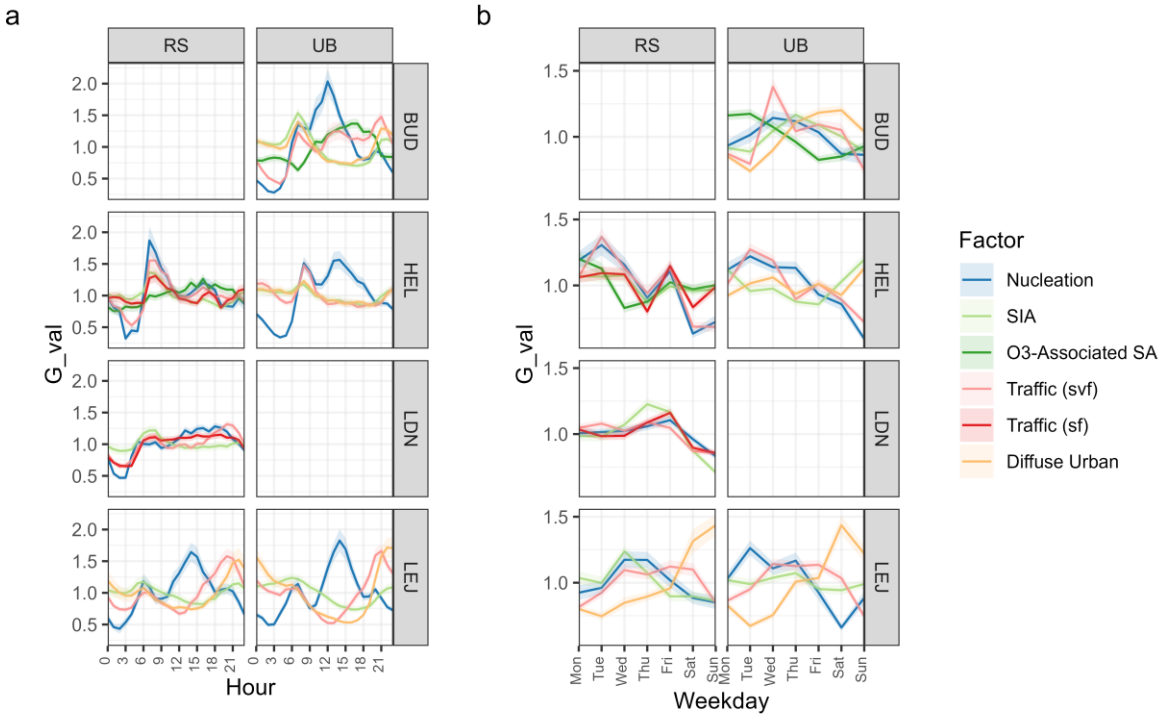

285 **Figure S4:** Mean G values from the PMF model for each factor, showing (a) daily and (b) weekly cycles. Each panel represents a factor and each colour represents a monitoring site. The shaded region represents the standard error of the mean.

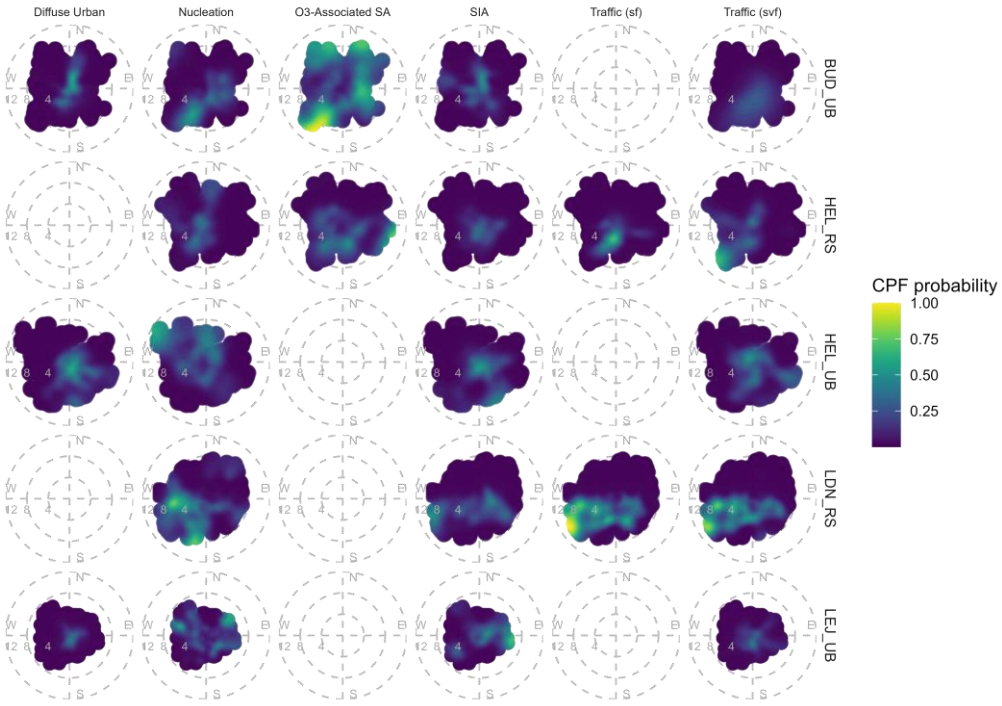

Figure S5: Polar plots showing the source regions most probable to produce the top 25th percentile of concentration as according to conditional probability function (CPF) analysis. Direction represents wind direction and distance from centre represents wind speed.

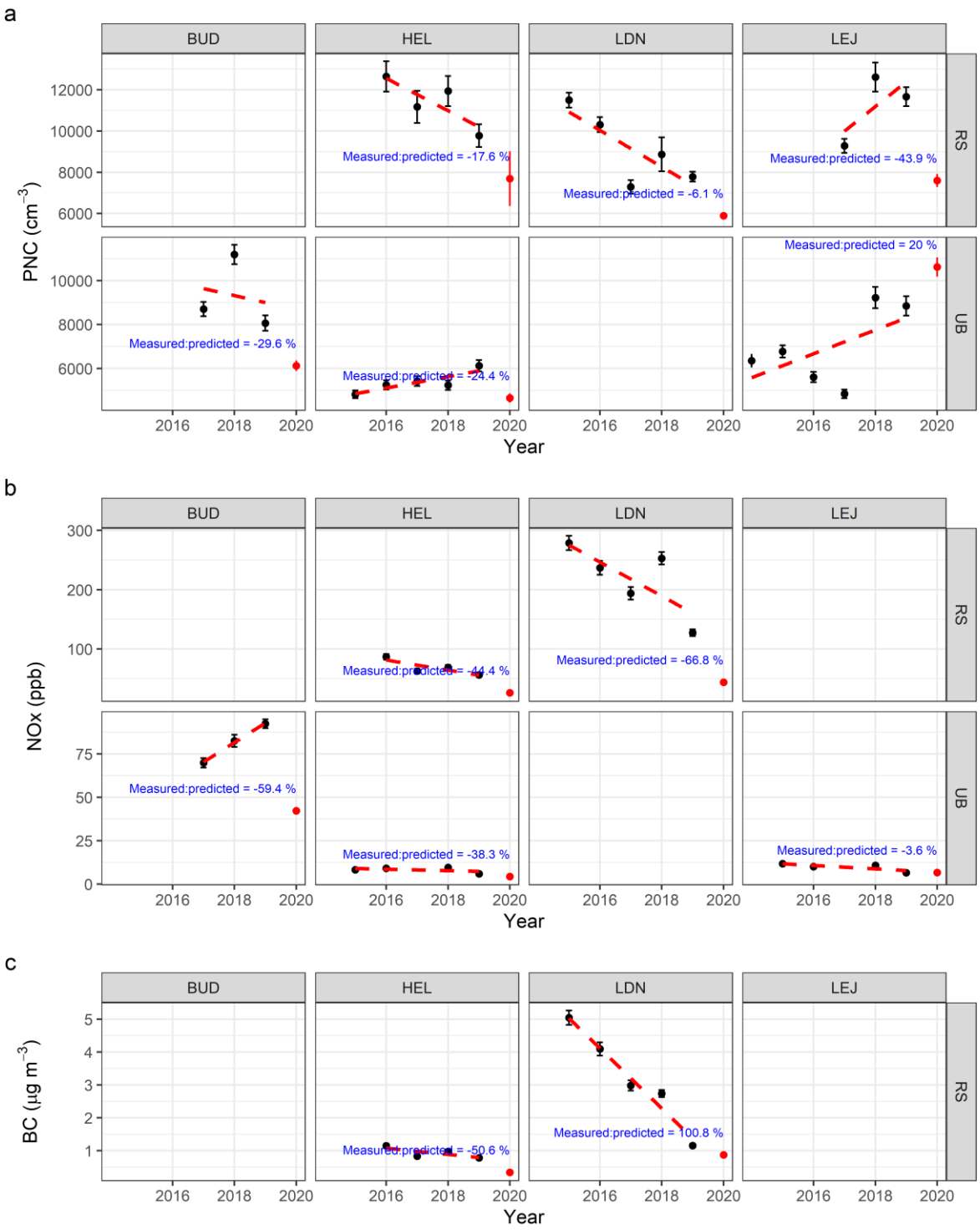

Figure S6: Linear regression analysis for each site, showing how (a) particle number concentrations (PNCs), (b) nitrogen oxides (NO_x), and (c) black carbon (BC) concentrations changed during lockdown (red dots) compared to the equivalent periods in the reference years (black dots), depending on data availability.

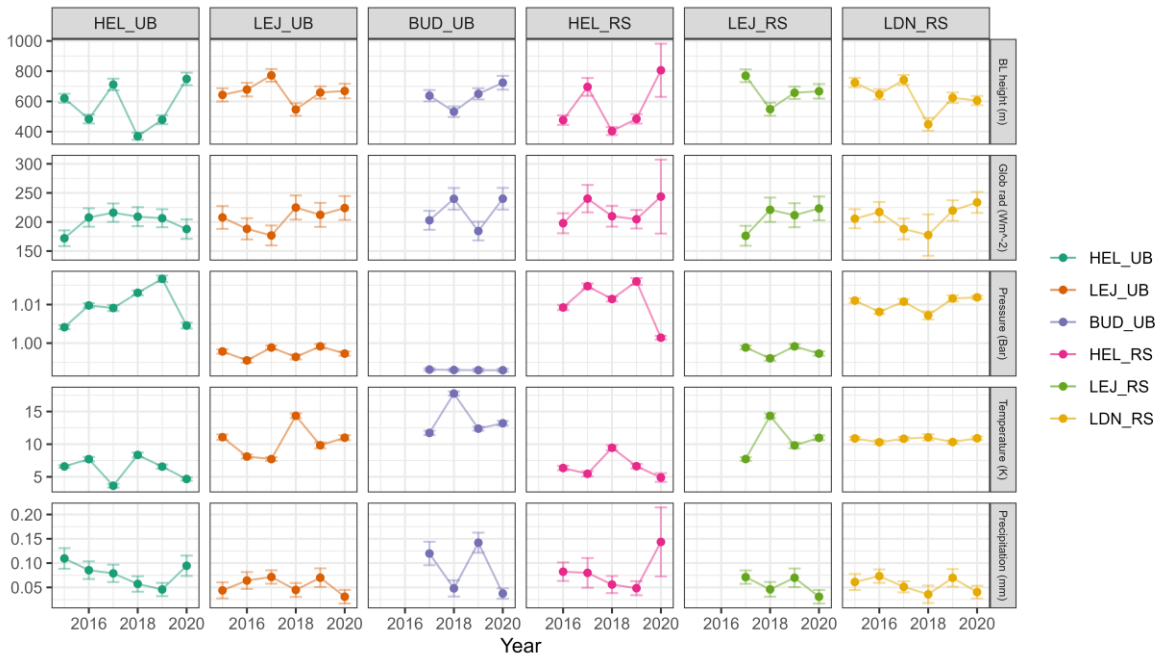

Figure S7: Means of meteorological variables from ERA5 during lockdown compared to the equivalent periods for previous years, for each site included in this study. Boundary layer height (BLH) = metres (m), global radiation = watts per square metre (W/m^2), atmospheric pressure = Bar, temperature = degrees Celsius (^oC), and precipitation = millimetres (mm).